NACA

RESEARCH MEMORANDUM

HIGH-SUBSONIC DAMPING-IN-ROLL CHARACTERISTICS OF A WING

WITH THE QUARTER-CHORD LINE SWEPT BACK 35° AND

WITH ASPECT RATIO 3 AND TAPER RATIO 0.6

By

Boyd C. Myers, II and Richard E. Kuhn

Langley Aeronautical Laboratory
Langley Air Force Base, Va.

NATIONAL ADVISORY COMMITTEE
FOR AERONAUTICS
WASHINGTON

May 10, 1949

NATIONAL ADVISORY COMMITTEE FOR AERONAUTICS

RESEARCH MEMORANDUM

HIGH-SUBSONIC DAMPING-IN-ROLL CHARACTERISTICS OF A WING

WITH THE QUARTER-CHORD LINE SWEPT BACK 35° AND

WITH ASPECT RATIO 3 AND TAPER RATIO 0.6

By Boyd C. Myers, II and Richard E. Kuhn

SUMMARY

An investigation of the damping-in-roll characteristics of a 35° swept-back wing, with and without vertical fins, has been made through a Mach number range of 0.40 to 0.91 in the Langley high-speed 7- by 10-foot tunnel utilizing a free-to-roll technique.

The damping-in-roll coefficient increased in magnitude with Mach number in the manner indicated by theory and generally was found to increase in magnitude with angle of attack over the range tested. Vertical fins located at about the midspan station of each wing panel had little effect on the damping-in-roll characteristics of the wing but increased the aileron effectiveness in producing rolling moment.

INTRODUCTION

An extensive investigation of the effects of compressibility on the damping-in-roll characteristics of various wing plan forms is being conducted in the Langley high-speed 7- by 10-foot tunnel. The 35° swept-back wing of aspect ratio 3 and taper ratio 0.6 employed in the present investigation was that used in the high-speed wind-tunnel investigation of the tailless model reported in reference 1. The present investigation was carried out on a free-rotating apparatus with the purpose of determining the effects of compressibility and angle of attack on the damping-in-roll characteristics of the wing, with and without the vertical fins that were used on the tailless model reported in reference 1.

COEFFICIENTS AND SYMBOLS

A   wing aspect ratio

a   speed of sound, feet per second

b   wing span (3.093 ft on model)

c   chord parallel to plane of symmetry

$\bar{c}$ mean aerodynamic chord (M.A.C.) (1.05 ft on model)

C_l rolling-moment coefficient $\left(\dfrac{\text{Rolling moment}}{qSb}\right)$

C_{l_p} damping-in-roll coefficient $\left(\dfrac{\partial C_l}{\partial \frac{pb}{2V}}\right)$

M   free-stream Mach number (V/a)

p   rate of roll, radians per second

q   dynamic pressure $(\rho V^2/2)$, pounds per square foot

R   Reynolds number $(\rho V \bar{c}/\mu)$

S   wing area (3.17 sq ft on model)

V   free-stream velocity, feet per second

ρ mass density of air, slugs per cubic foot

μ absolute viscosity, pound-seconds per square foot

α angle of attack, degrees

δ control-surface deflection with reference to wing-chord line
               parallel to plane of symmetry; positive deflection
               down, degrees

pb/2V   wing-tip helix angle, radians

$$C_{l_\delta} = \frac{\partial C_l}{\partial \delta}$$

$$(pb/2V)_\delta = \frac{\partial \frac{pb}{2V}}{\partial \delta}$$

Subscripts:

a_l left aileron

a_r right aileron

MODEL AND APPARATUS

The pertinent dimensions of the steel wing, ailerons, and vertical fins are given in figure 1. The ailerons were of true contour and constant chord and had sealed-nose gaps. The ordinates of the symmetrical airfoil section, which is not a standard NACA section, are given in table I.

The model was supported by a sting extending forward into the test section from a vertical strut located behind the model. The vertical strut was part of the wind-tunnel balance system and both the strut and a portion of the sting were shielded from the air stream by a fairing. A schematic drawing of the support system and rolling apparatus is shown in figure 2. The angle of attack of the model was changed by varying the angle of incidence of the wing relative to the sting. This was accomplished by utilizing various incidence blocks fitted into the sting. A photograph of the installation is shown in figure 3. The rolling-moment data were obtained from wind-tunnel balance measurements with the sting restrained in roll. When the model was permitted to roll freely under the moment created by the deflected aileron, the rate of roll was recorded electrically.

TESTS AND PROCEDURE

Scope

The model was tested in two configurations, fins off and fins on, through a Mach number range of 0.40 to 0.91. The fins-off configuration was tested through an angle-of-attack range from 0.30° to 6.50°; whereas, the fins-on configuration was tested only at an angle of attack of 0.30°. However, both configurations were tested through an aileron-deflection range of 0° to $\pm9.4^\circ$ and only the left aileron was deflected.

The size of the model used in the present investigation resulted in an estimated choking Mach number of 0.94 and the data are believed to be reliable to a corrected Mach number of about 0.91. The variation of test Reynolds number with Mach number for average test conditions is presented in figure 4.

Corrections

A small tare correction in the form of bearing friction was applied to the results as an increment of damping-in-roll coefficient equal to -0.005. The rolling-moment coefficients and Mach numbers have been corrected for blocking by the model and its wake, by the method of reference 2.

Reduction of Data

The coefficient of damping in roll C_{l_p} is defined as follows:

$$C_{l_p} = \frac{\partial C_l}{\partial \frac{pb}{2V}} = - \frac{C_{l_\delta}}{\left(\frac{pb}{2V}\right)_\delta}$$

where the expressions C_{l_δ} and $(pb/2V)_\delta$ were evaluated graphically as the slopes of the curves of the rolling-moment coefficient C_l plotted against aileron deflection δ and of the nondimensional steady rate of rolling $(pb/2V)$ plotted against aileron deflection δ, respectively.

RESULTS AND DISCUSSION

The results are presented in the following figures:

	Figure
Basic force data C_l plotted against M	
Fins off	5
Fins on	6
Basic rolling data $\frac{pb}{2V}$ plotted against M	
Fins off	7
Fins on	8
Summary data	
Aileron effectiveness C_{l_δ} and $\left(\frac{pb}{2V}\right)_\delta$ plotted against M	
Fins off	9
Fins on	10
Damping-in-roll coefficient C_{l_p} plotted against M	
Fins off	11
Fins on	12

The variation of the damping-in-roll coefficient C_{l_p} with Mach number is presented in figure 11 and the effect of fins is presented in figure 12. It will be noted that the experimental variation of C_{l_p} with Mach number (fig. 11) agrees fairly well with theory (reference 3), although the absolute values of the damping coefficients are slightly greater than the theoretical values. The increase in the magnitude of C_{l_p} with angle of attack, which is evident from figure 11, (particularly at the high Mach numbers) is not accounted for in the basic theory as ordinarily applied. However, experimental data on a similar wing (reference 4) gave a similar variation of C_{l_p} with angle of attack. The slight reduction in magnitude of C_{l_p} at 1.8° angle of attack may be caused by a local change in the section lift-curve slope. Reference 5 indicates that C_{l_p} of a wing is approximately proportional to the slope of the section lift-curve slope at any particular angle of attack. However, since the actual section lift characteristics for this airfoil are not available, no analysis has been made to check this effect.

The effect of the fins on the damping coefficient was almost negligible (fig. 12). However, the addition of the vertical fins produced a marked increase in the effectiveness of the ailerons in producing both rolling moment and rolling velocity (fig. 10). This effect can probably be attributed to the end-plate effect of the fins.

CONCLUSIONS

The results of an investigation of the effects of Mach number and angle of attack on the damping-in-roll characteristics of a 35° swept-back wing of aspect ratio 3 and taper ratio 0.6 indicate the following conclusions:

1. The damping-in-roll derivative C_{l_p} increased in magnitude gradually with Mach number in a manner similar to that predicted from theory.

2. The damping-in-roll derivative C_{l_p} generally increased in magnitude with angle of attack within the test range, especially at higher Mach numbers.

3. Vertical fins, mounted at approximately the midspan section of
each wing panel, had little effect on the damping-in-roll characteristics
of the wing but increased the effectiveness of the ailerons in producing
rolling moment.

Langley Aeronautical Laboratory
        National Advisory Committee for Aeronautics
   Langley Air Force Base, Va.

REFERENCES

1. Donlan, Charles J., and Kuhn, Richard E.: Estimated Transonic Flying
        Qualities of a Tailless Airplane Based on a Model Investigation.
        NACA RM No. L9D08, 1949.

2. Herriot, John G.: Blockage Corrections for Three-Dimensional-Flow
        Closed-Throat Wind Tunnels, with Consideration of the Effect of
        Compressibility. NACA RM No. A7B28, 1947.

3. Bird, John D.: Some Theoretical Low-Speed Span Loading Characteristics
        of Swept Wings in Roll and Sideslip. NACA TN No. 1839, 1949.

4. Queijo, M. J., and Lichtenstein, Jacob H.: The Effects of High-Lift
        Devices on the Low-Speed Stability Characteristics of a
        Tapered 37.5° Sweptback Wing of Aspect Ratio 3 in Straight and
        Rolling Flow. NACA RM No. L8I03, 1948.

5. MacLachlan, Robert, and Letko, William: Correlation by Two
        Experimental Methods of Determining the Rolling Characteristics of
        Unswept Wings. NACA TN No. 1309, 1947.

TABLE I.- ORDINATES OF SYMMETRICAL

AIRFOIL SECTION

[All dimensions in percent of wing chord
parallel to plane of symmetry of wing]

Station, x	Ordinate, ±y
0	0
.5871	1.0958
.8803	1.3226
1.4661	1.6687
2.9264	2.2597
5.8297	2.9981
8.7103	3.4923
11.5680	3.8626
17.2154	4.3929
22.7728	4.7516
28.2409	4.9951
33.6203	5.1488
38.9118	5.2322
44.1160	5.2200
49.2336	5.1300
54.2654	4.9088
59.2118	4.5506
64.0736	4.0784
68.9587	3.5320
73.5461	2.9550
78.1583	2.3821
82.6881	1.8395
87.1366	1.3383
91.5043	.8757
95.7921	.4408
100.0000	.0206

NACA
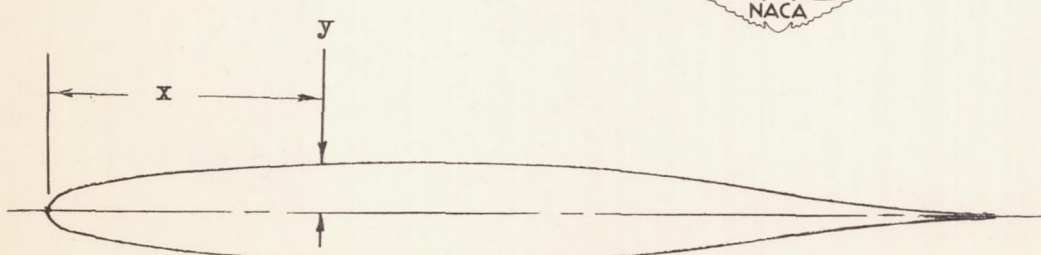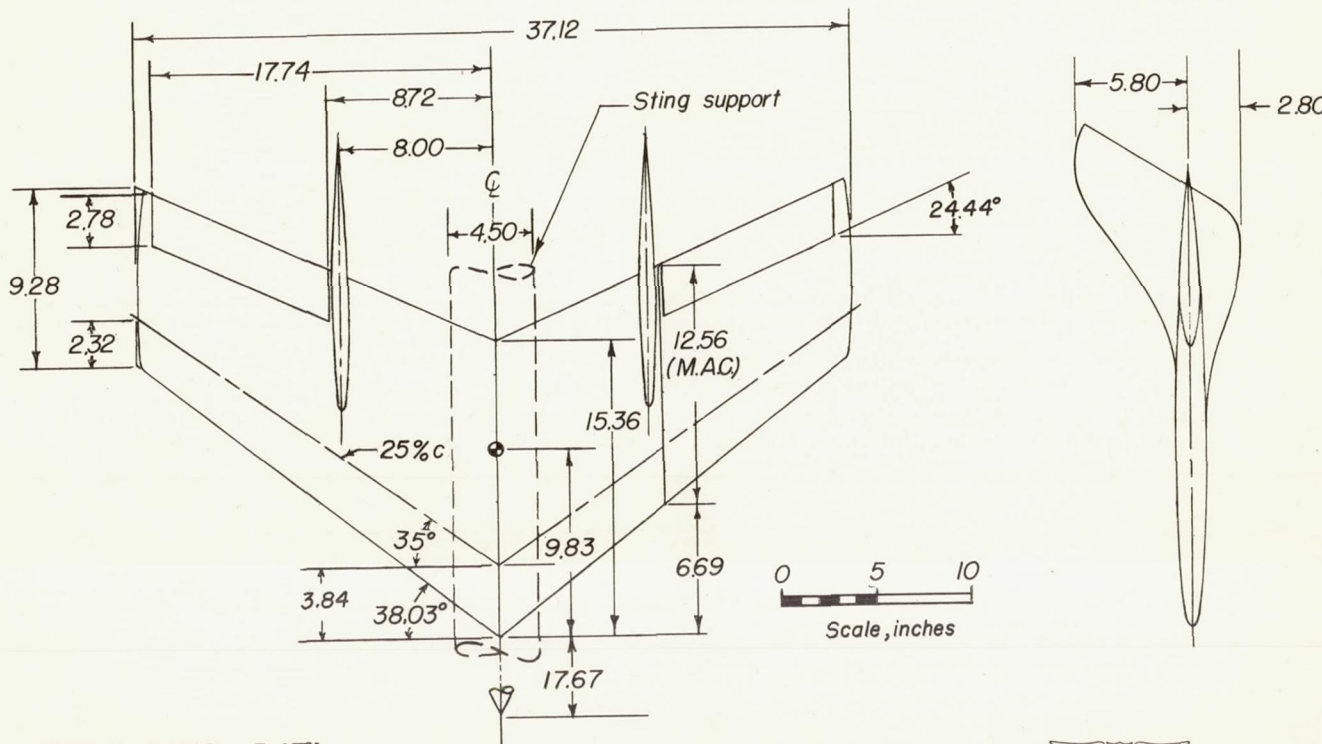
TABULATED DATA

Wing

Area	3.17 sq ft
Aspect ratio	3.0
Mean aerodynamic chord	1.05 ft
Dihedral	0°
Taper ratio	0.6
Airfoil (Table I)	symmetrical
Location of max. thickness	0.39c
Maximum thickness	0.105c

Vertical fins

Area (two)	0.82 sq ft
Aspect ratio	1.75
Moment reference point	0.25 M.A.C.

Ailerons

Area (two)	0.348 sq ft
Sweep, hinge axis	24.44°

Figure 1.- Drawing of test wing and vertical fins.
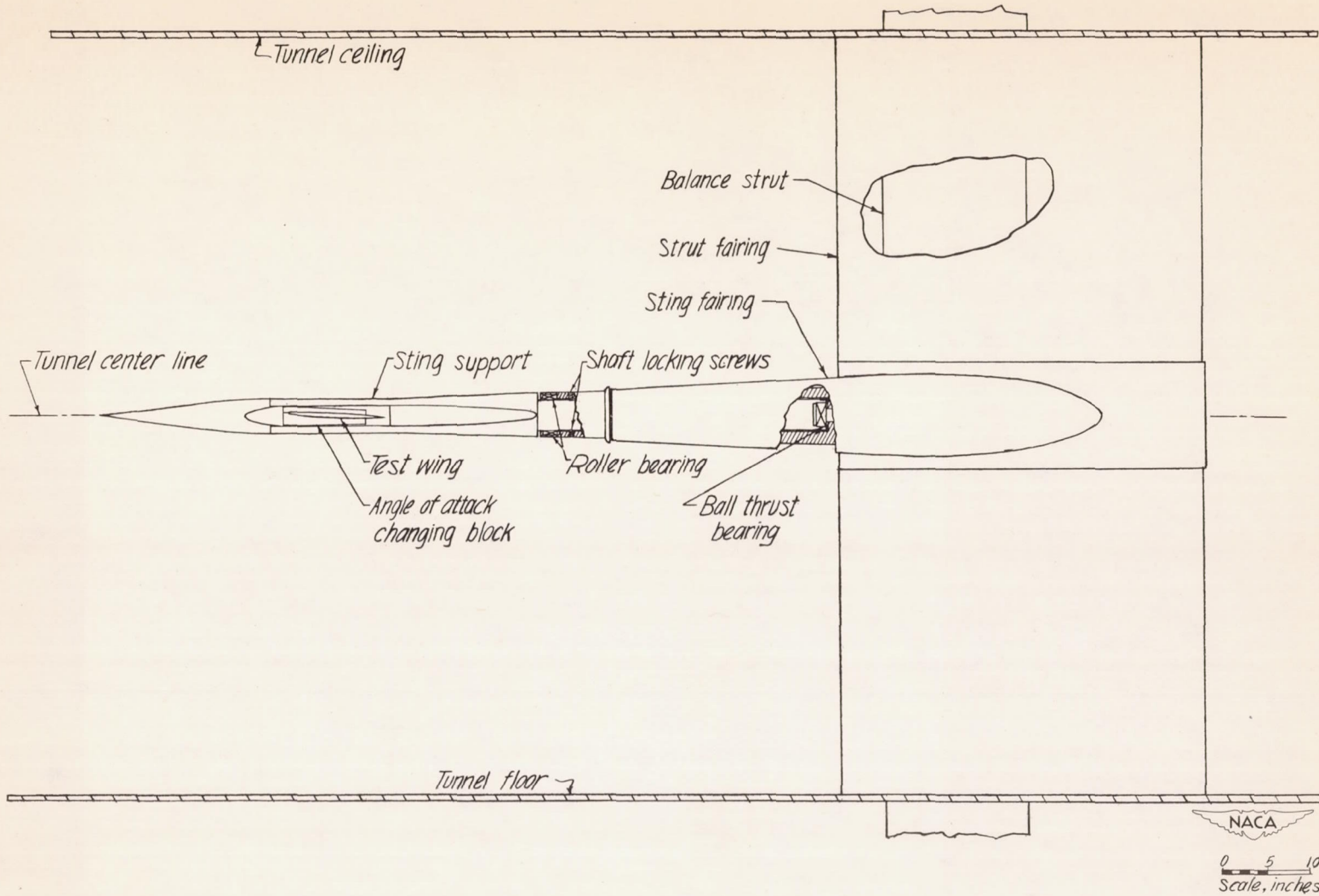
Figure 2.- Schematic drawing of the free-rolling sting mounted in the Langley high-speed 7- by 10-foot tunnel test section.
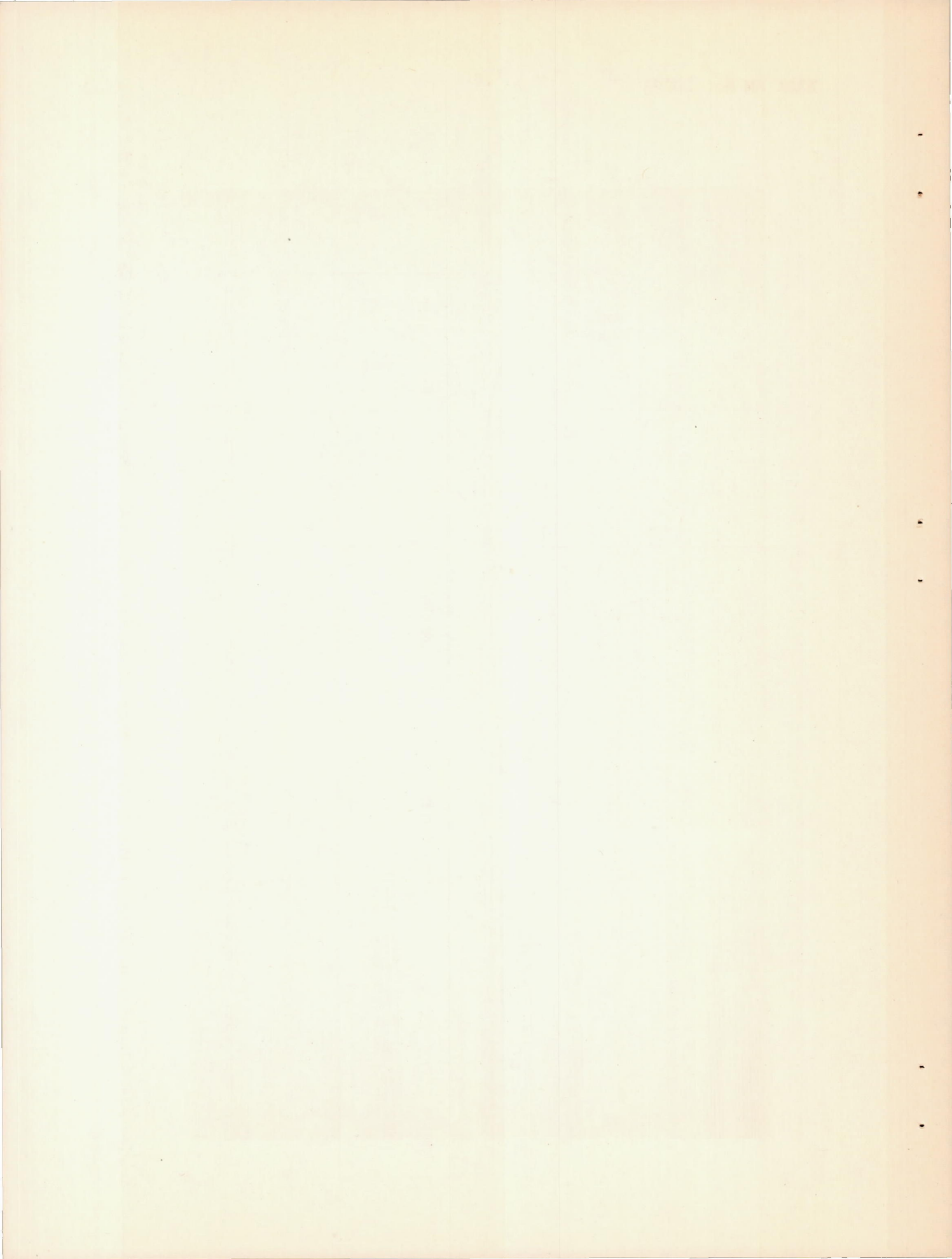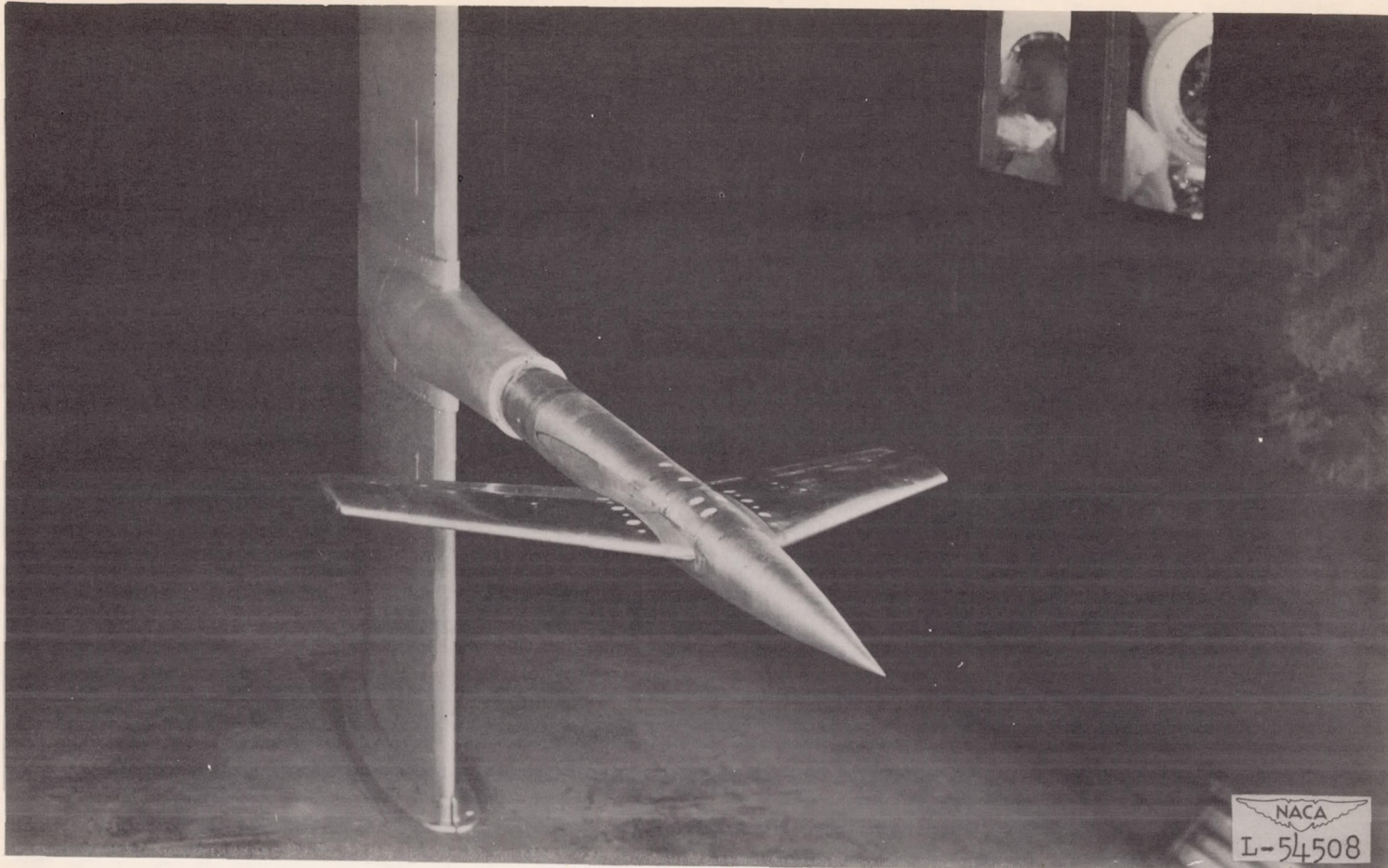
Figure 3.- Photograph of the test wing, vertical fins off, mounted on the free-rolling sting in the Langley high-speed 7- by 10-foot tunnel test section.
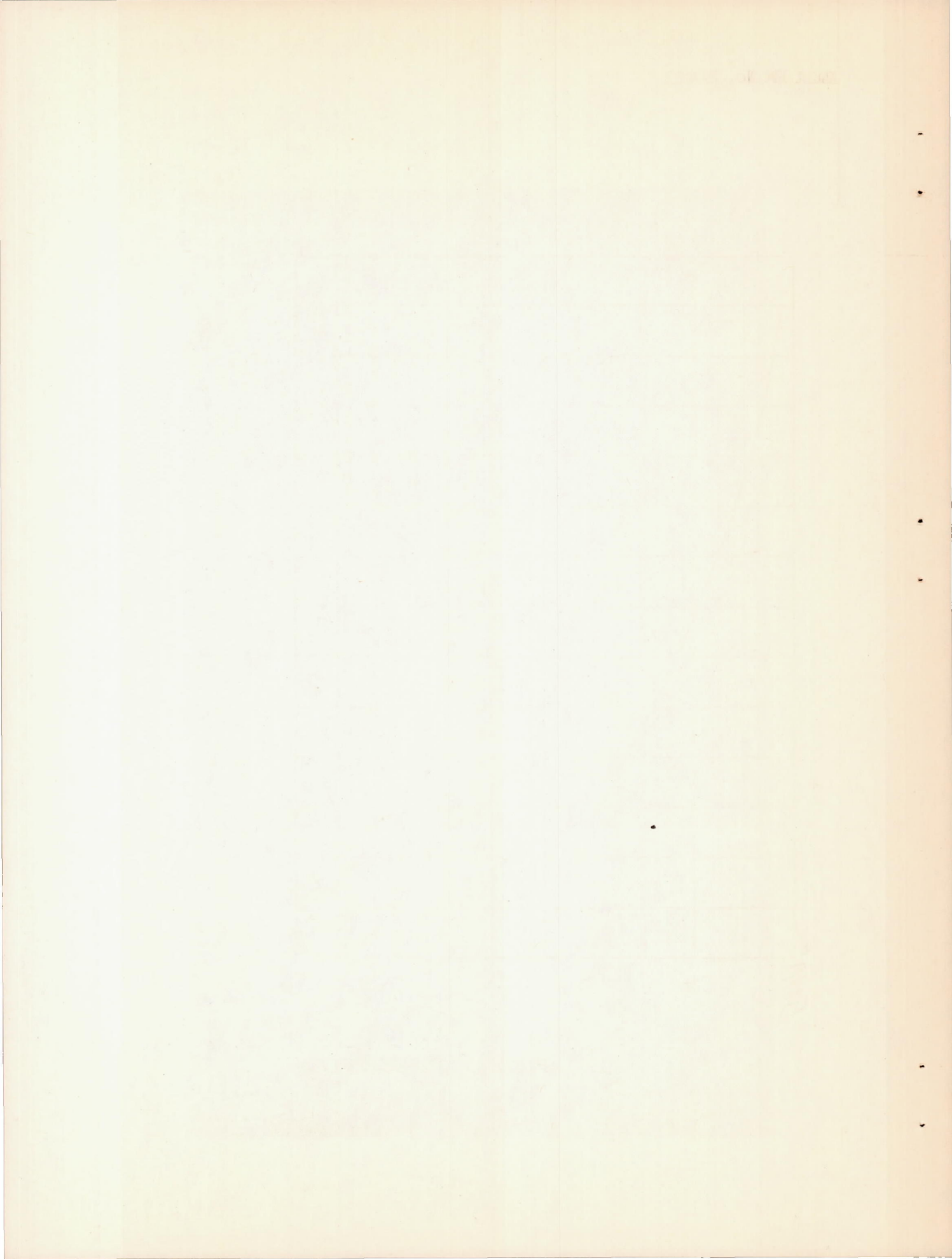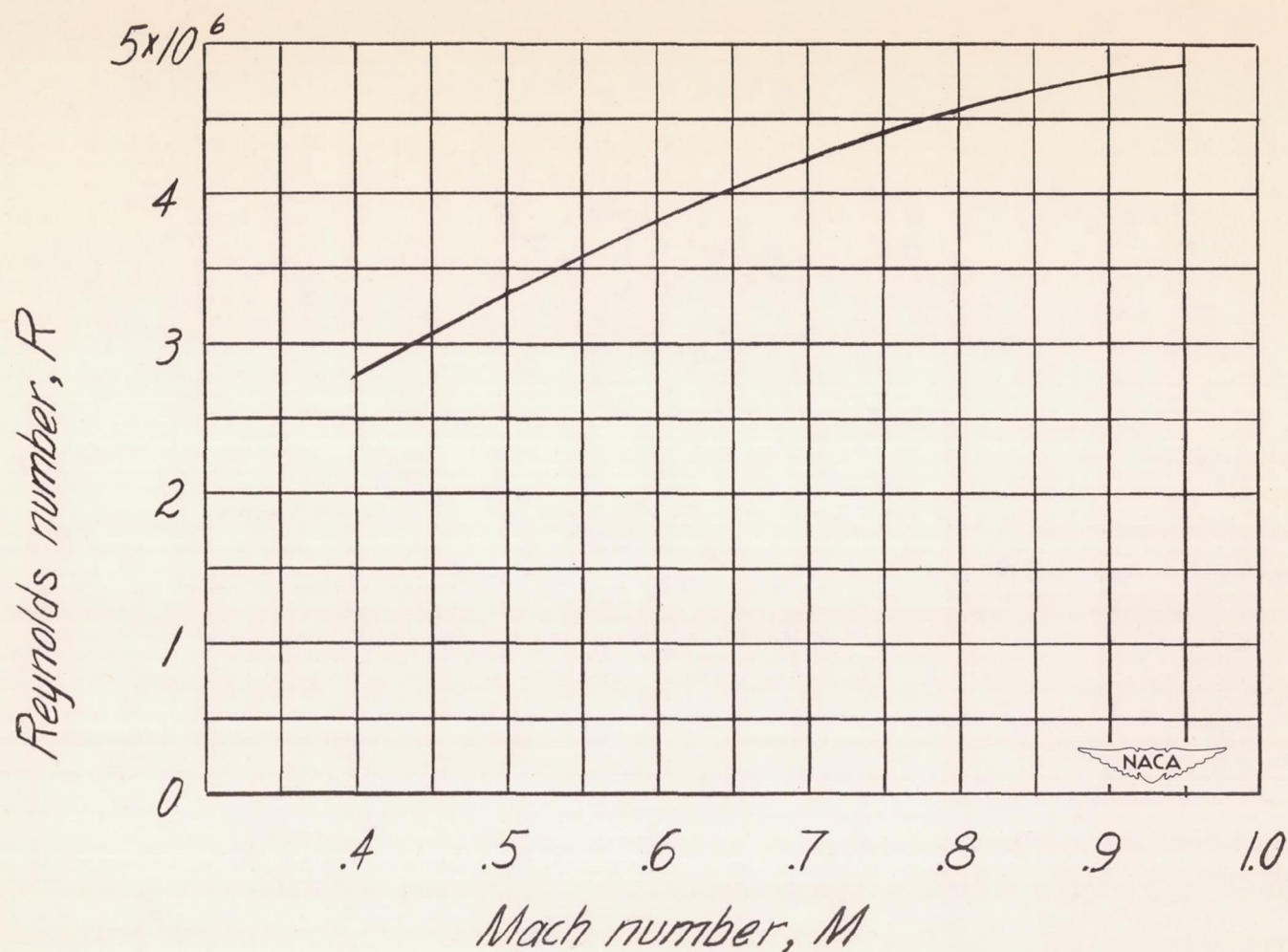
Figure 4.- Variation of test Reynolds number with Mach numbers based on the mean geometric chord of 1.046 feet.
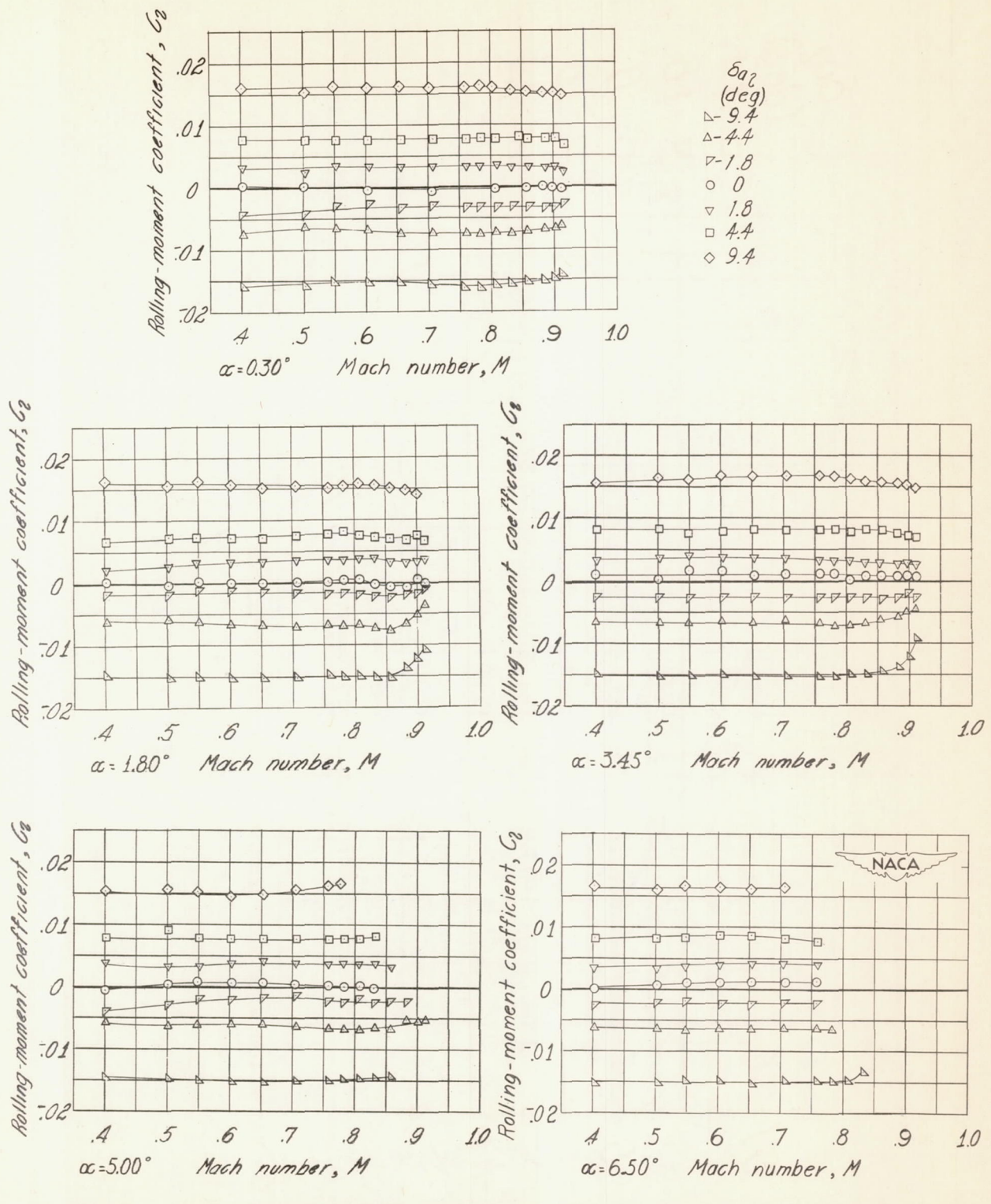
Figure 5.- Variation with Mach number of the rolling-moment characteristics
of the test wing for various angles of attack and aileron deflections;
vertical fins off; $\delta_{a_r} = 0$.
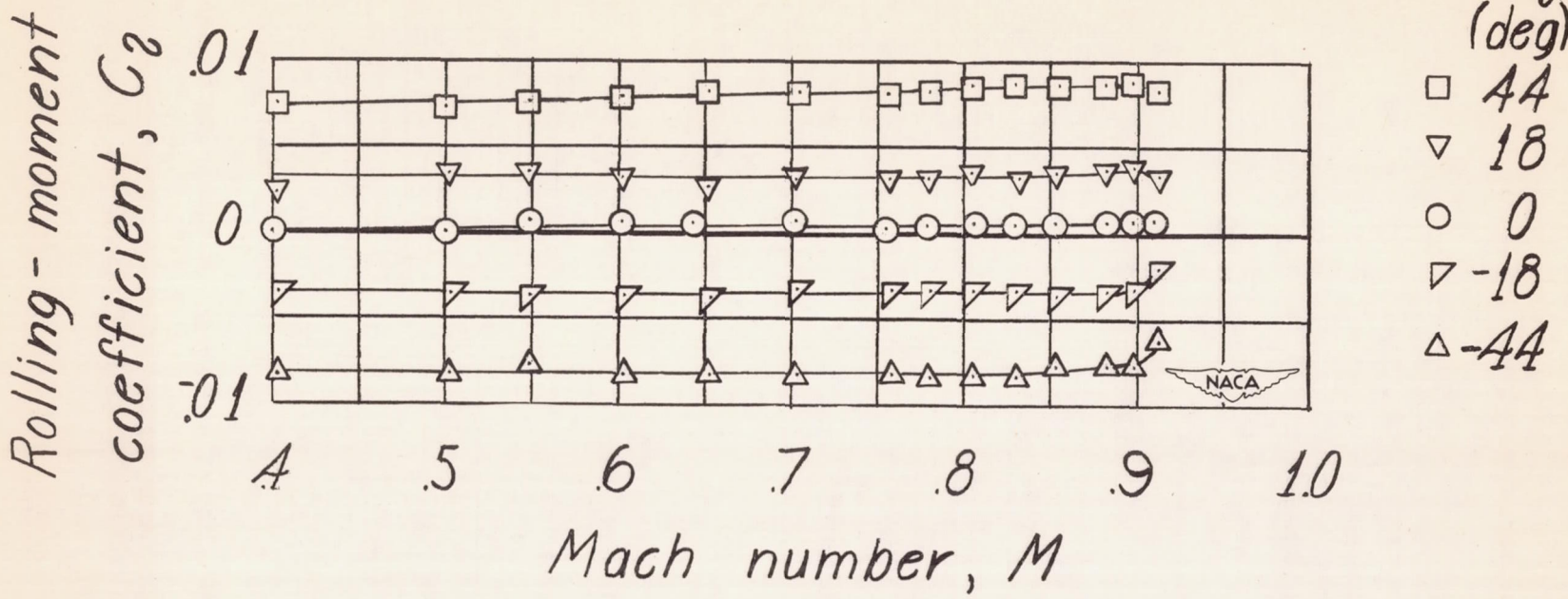
Figure 6.- Variation with Mach number of the rolling-moment characteristics of the test wing, $\alpha = 0.30^\circ$; vertical fins on; $\delta_{a_r} = 0$.
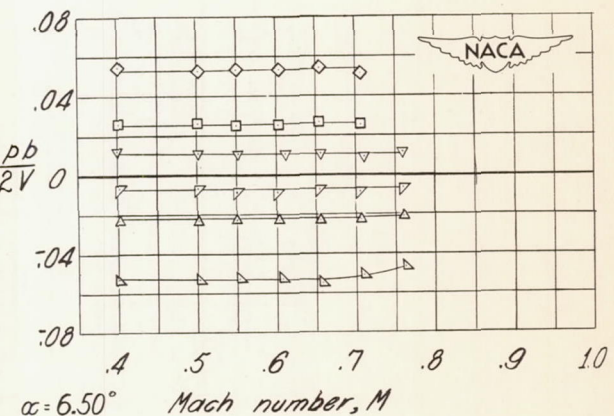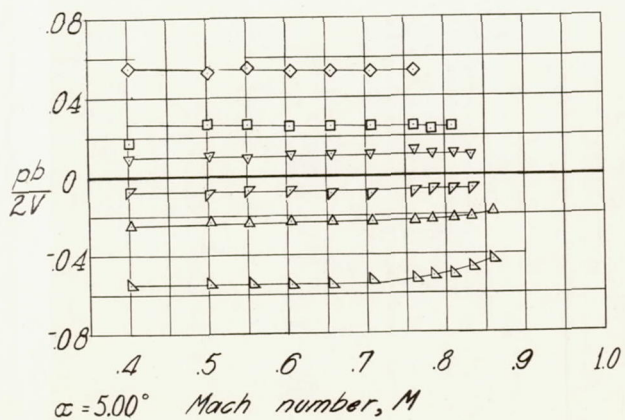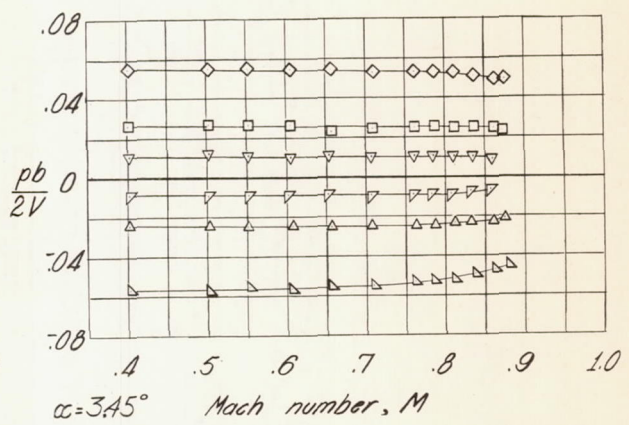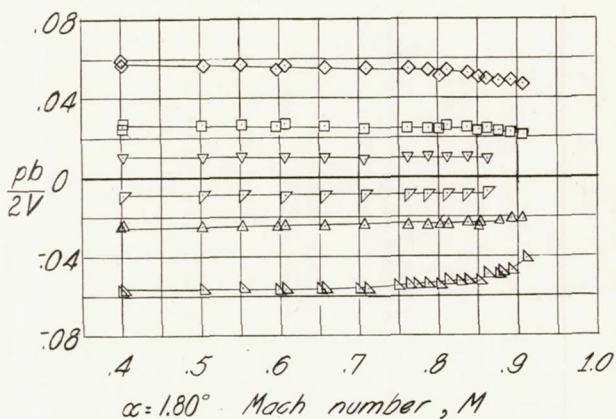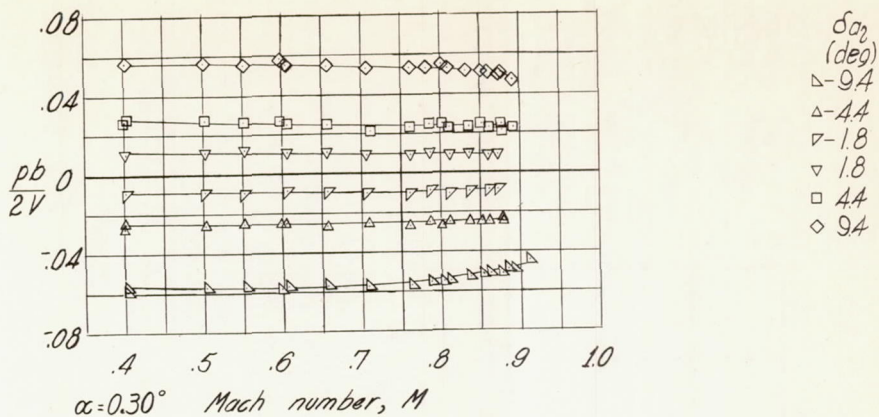
Figure 7.- Effect of Mach number on the wing-tip helix angle obtained for several angles of attack with various aileron deflections; vertical fins off; $\delta_{a_r} = 0$.
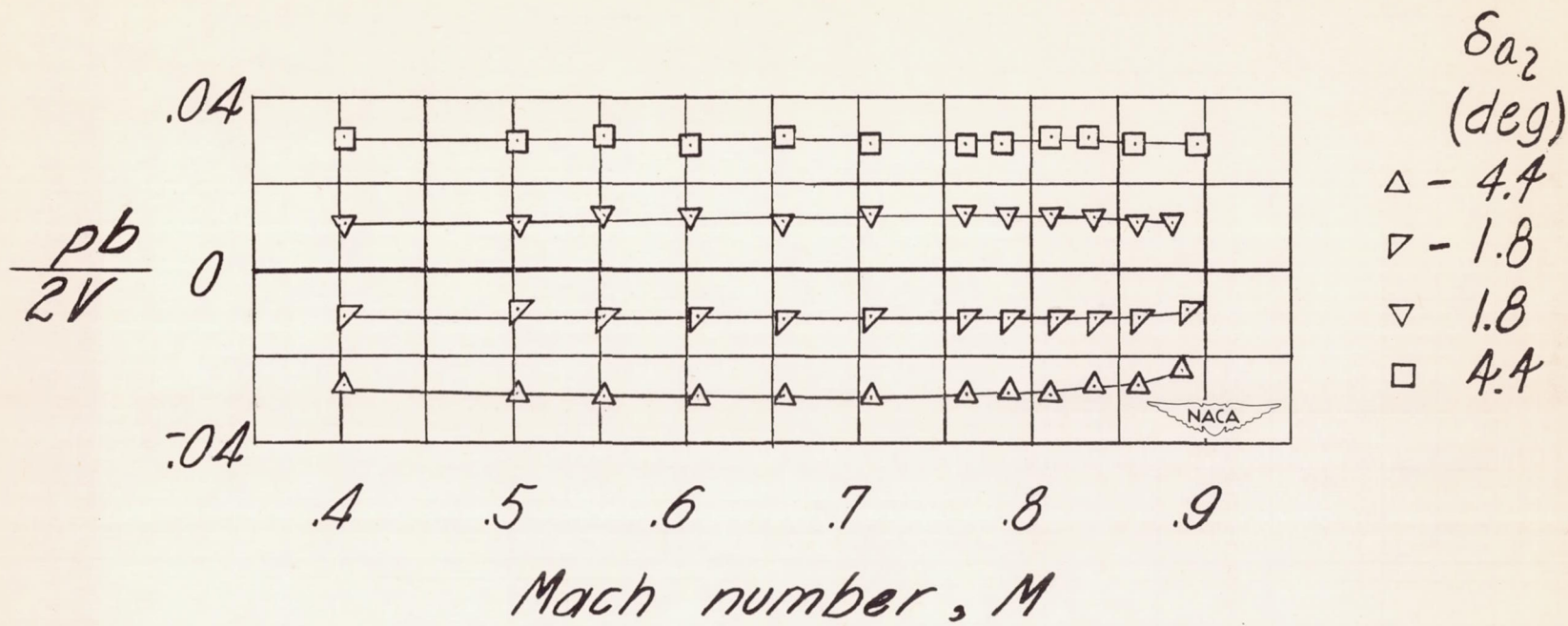
Figure 8.- Variation with Mach number of the wing-tip helix angle obtained for various aileron deflections; vertical fins on; $\delta_{a_r} = 0$.
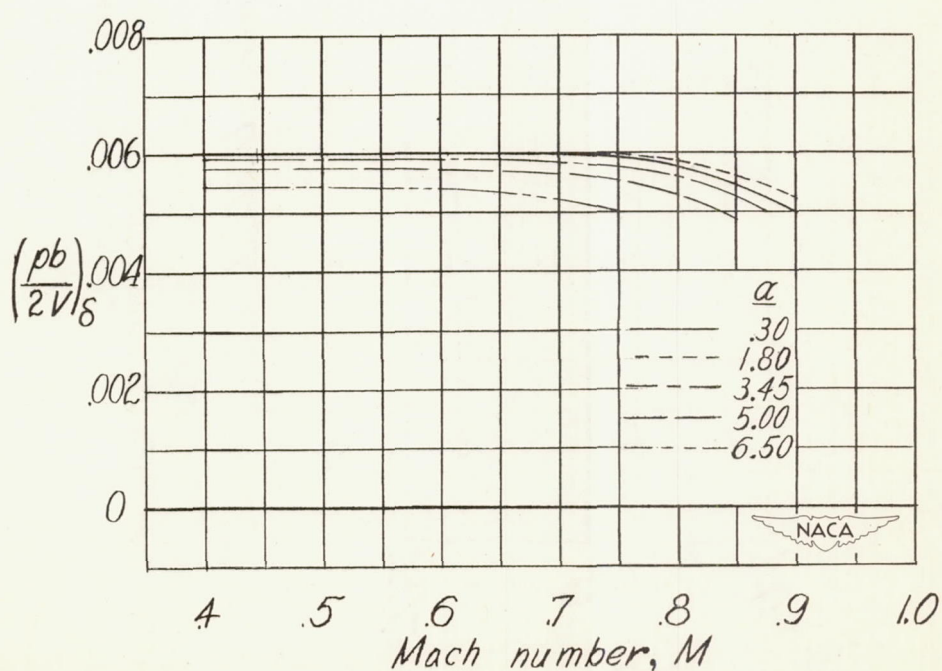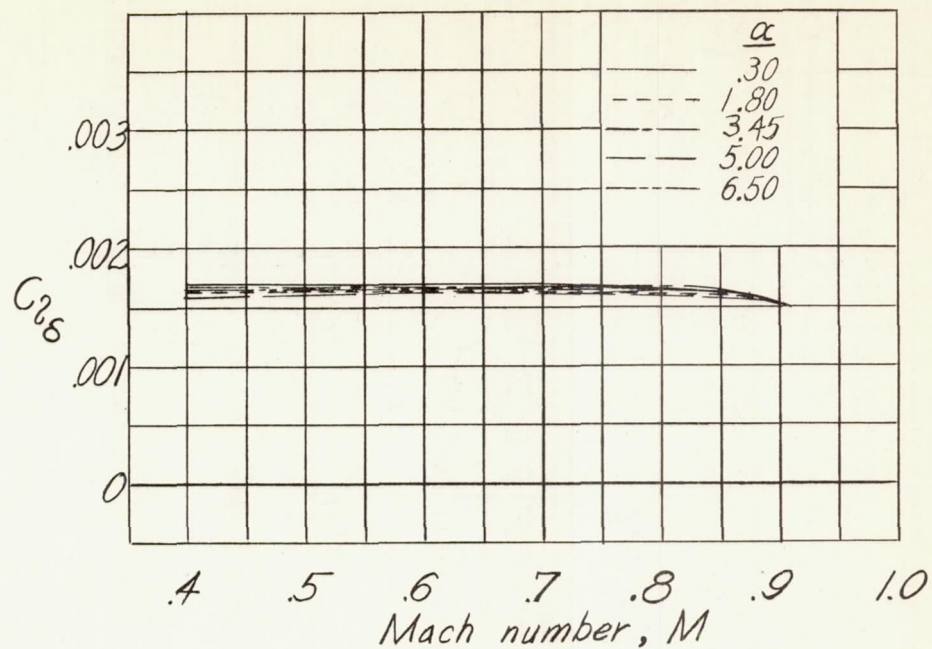
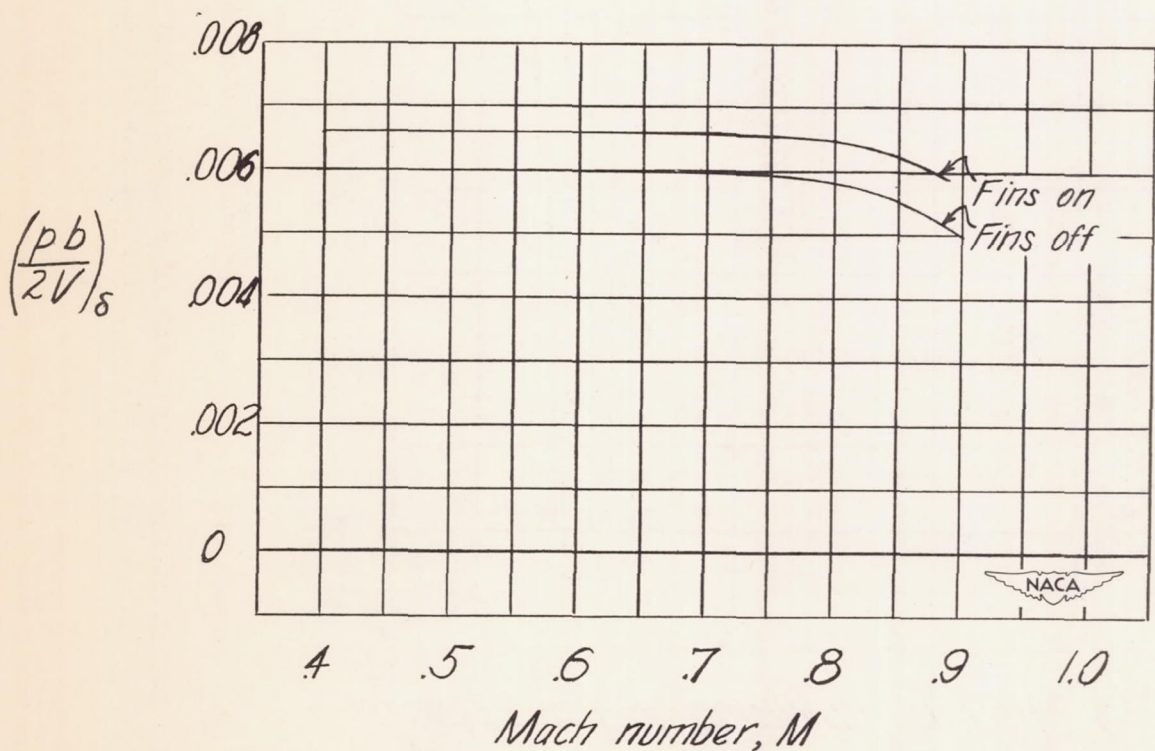Figure 9.- Variation of the aileron effectiveness with Mach number for various angles of attack; vertical fins off.
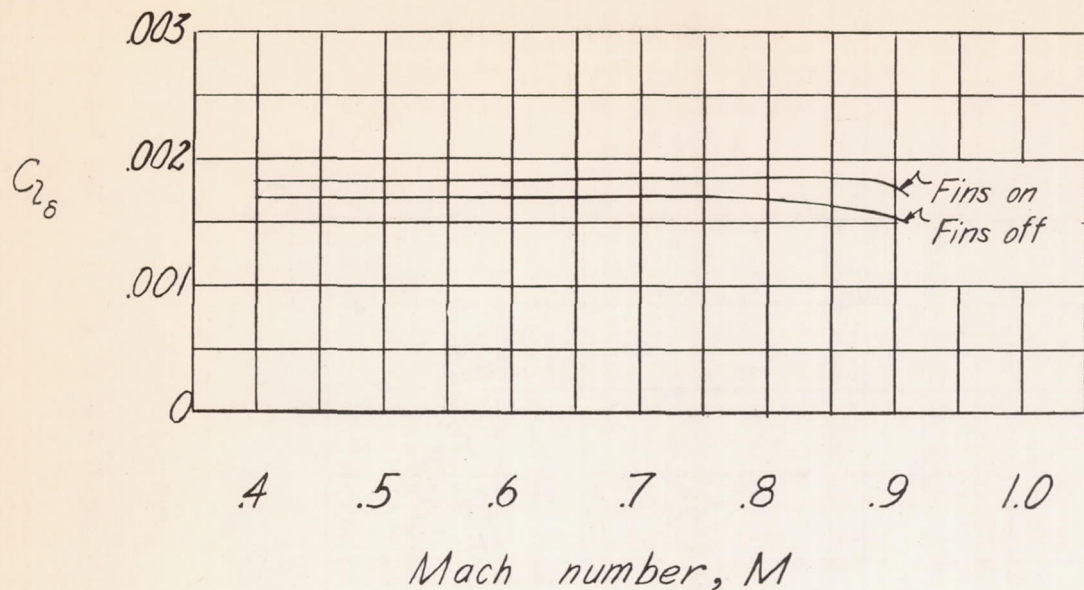
Figure 10.- Effect of the vertical fins on the aileron effectiveness;
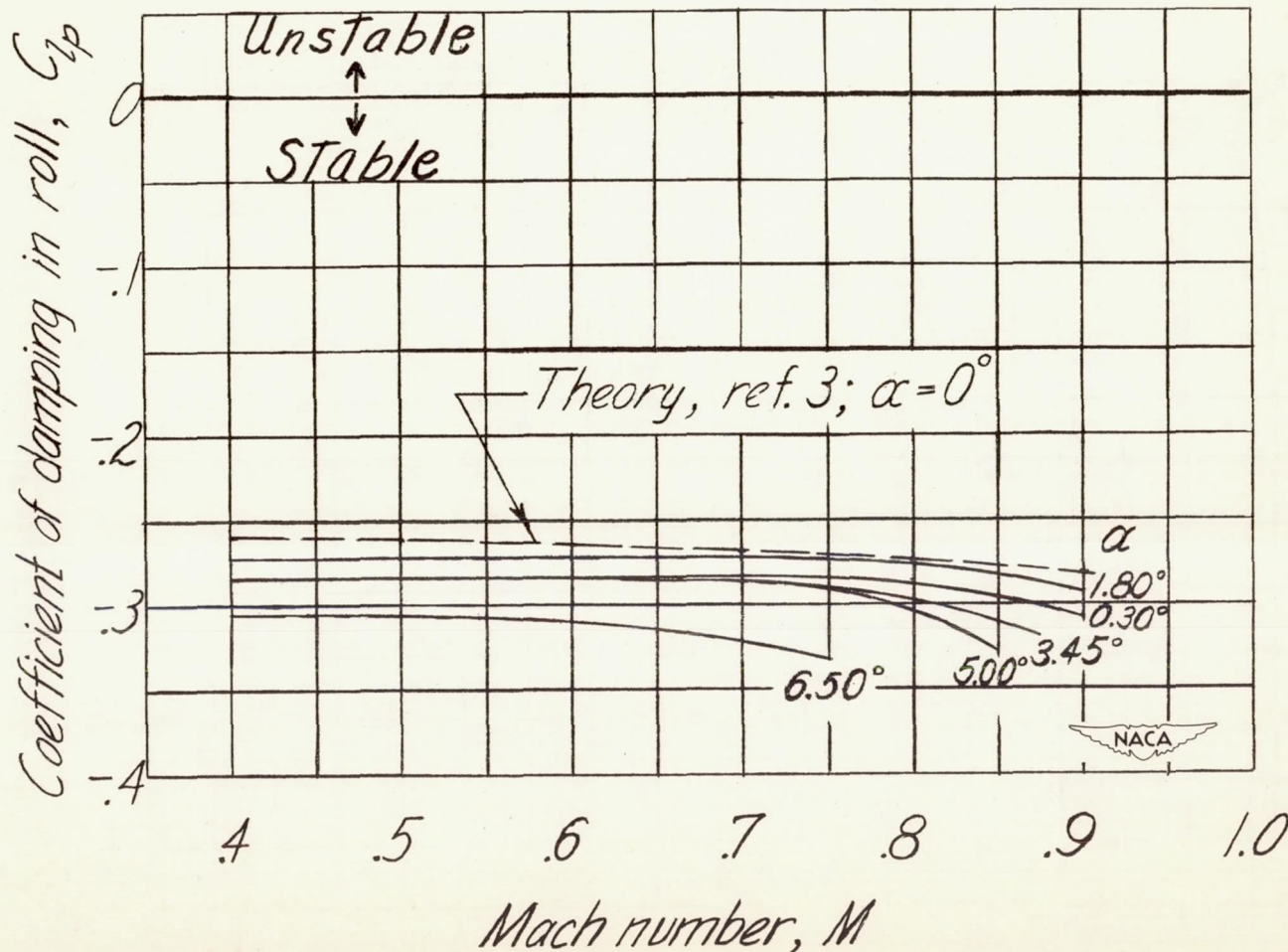$\alpha = 0.30^\circ$.

Figure 11.- Variation of the coefficient of damping in roll C_{l_p} with Mach number for various angles of attack; vertical fins off.
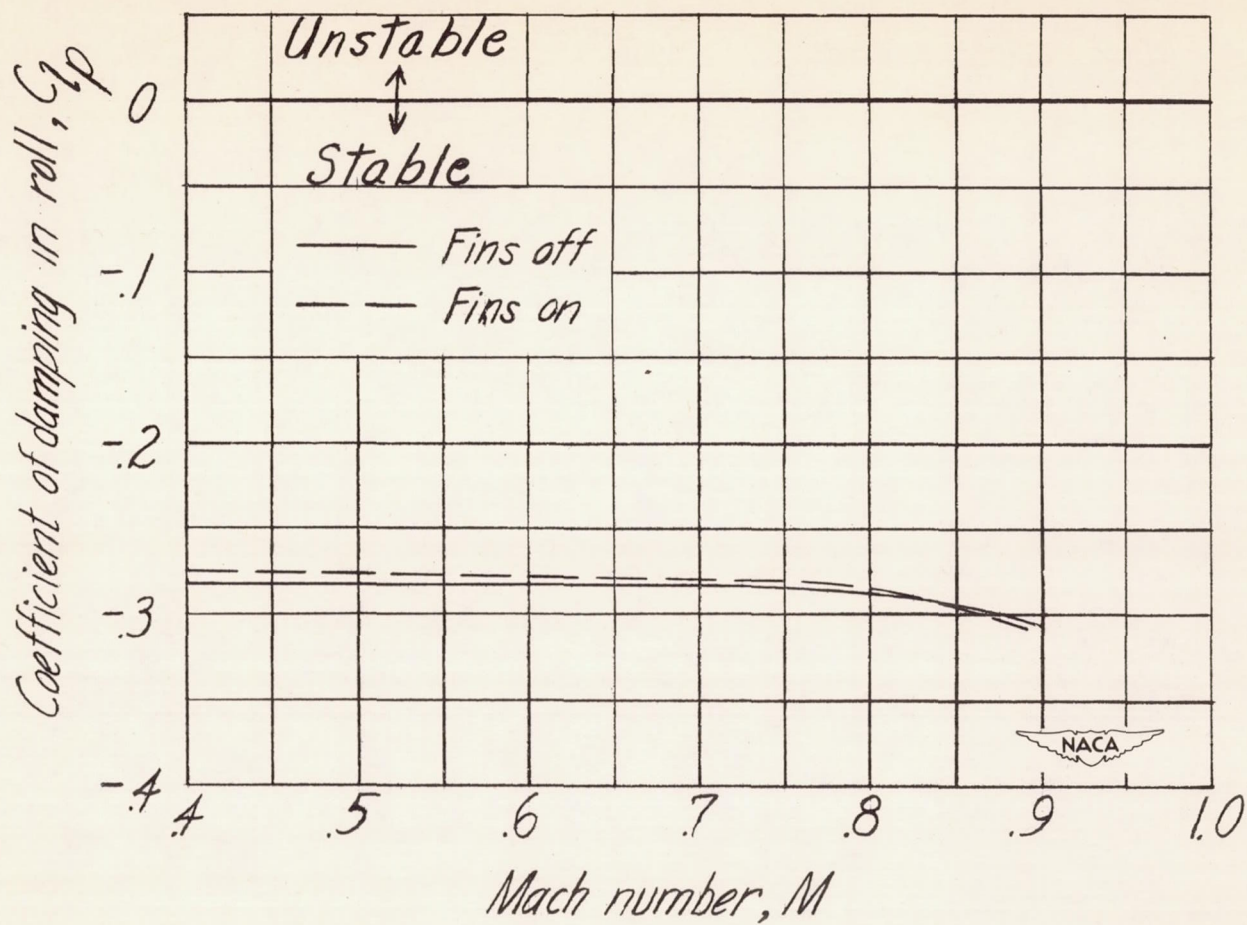
Figure 12.- Effect of the vertical fins on the coefficient of damping in roll C_{l_p}; $\alpha = 0.30°$.